Periodic orbit quantization of the anisotropic Kepler problem

Freddy Christiansen and Predrag Cvitanović
Niels Bohr Institute, Blegdamsvej 17, DK-2100 Copenhagen Ø, Denmark

(Received 20 October 1991; accepted for publication 7 January 1992)

The periodic orbit quantization on the anisotropic Kepler problem is tested. By computing the stability and action of some 2000 of the shortest periodic orbits, the eigenvalue spectrum of the anisotropic Kepler problem is calculated. The aim is to test the following claims for calculating the quantum spectrum of classically chaotic systems: (1) Curvature expansions of quantum mechanical zeta functions offer the best semiclassical estimates; (2) the real part of the cycle expansions of quantum mechanical zeta functions cut at appropriate cycle length offer the best estimates; (3) cycle expansions are superfluous; and (4) only a small subset of cycles (irreducible cycles) suffices for good estimates for the eigenvalues. No evidence is found to support any of the four claims.

I. INTRODUCTION

At first glance, the anisotropic Kepler problem seems to be the ideal testing ground for periodic orbit quantization of bound systems, indeed, so ideal that Martin Gutzwiller has asked us to convince him of the utility of the cycle expansion techniques by demonstrating that their accuracy surpasses his original calculation[1] of the anisotropic Kepler problem spectrum.

In this contribution to this issue of CHAOS, we present cycle expansion spectra computations based on the evaluation of thousands of cycles. In the cycling business, one aims for many decades of extra precision over that attainable by trace formulas; as the accuracy of our spectra is still not significantly better than Gutzwiller's, the original gentleman's agreement is hereby breached. Our hand is forced by the proceeding paper,[2] and the hope that the failure is instructive if it clarifies the nature of the obstacle. Our purpose is to test the following claims that have animated much of the discussions of the Nordita 1991 Quantum Chaos workshop.

(1) The complex zeros of the curvature expansions of quantum mechanical zeta functions offer, at present, the best semiclassical estimates of the low eigenvalues of classically chaotic quantum systems.[3]

(2) The best estimate for low eigenvalues of classically chaotic quantum systems is obtained by taking the real part of the cycle expansion of the quantum mechanical zeta function, cut at appropriate cycle length.[4]

(3) Cycle expansions are superfluous; the real part of the truncated Selberg product for the quantum mechanical zeta function yields a better semiclassical estimate for the low eigenvalues.[5]

(4) Only a small subset of cycles suffices for good estimates of the eigenvalues up to a given cutoff energy.[6]

Here, we shall test claim (4) on a simple one-dimensional system; we find no numerical evidence in its support. The remaining claims are tested on the anisotropic Kepler problem; the results are not more encouraging.

II. ANISOTROPIC KEPLER PROBLEM

The anisotropic Kepler problem appears ideal for testing the validity of quantum cycle expansions because Gutzwiller[1] has provided strong evidence that for anisotropies as large as the physically interesting ones, all cycles (computed so far) are unstable, and in one-to-one correspondence with a simple symbolic dynamics. For a Hamiltonian system, such a claim is very surprising; we know of no other example of a bound Hamiltonian system with simple symbolic dynamics, and this makes the anisotropic Kepler problem the unique candidate for testing cycle expansions. For simple symbolic dynamics, the cycles can be combined into "shadowed" curvature combinations, and cycle expansions are expected to converge well. However, as we shall see, the real difficulty with the anisotropic Kepler problem was unanticipated; such "naive" shadowing of long orbits by short ones fails.

The anisotropic Kepler problem is discussed in depth in Gutzwiller's monograph,[1] whose notational conventions we follow here. Briefly, the anisotropic Kepler problem has its experimental background in solid state physics. Electrons associated with donor impurities in silicon and germanium lattices have an anisotropic effective mass tensor, with the anisotropy defined as the ratio μ/ν between the high and the low components. For silicon, this ratio is $\mu/\nu = 4.810$ and, for germanium, it is $\mu/\nu = 19.48$ (Ref. 7). If the only force comes from the donor impurity, the problem can be approximated by the effective Hamiltonian

$$E = \frac{p_x^2}{2\mu} + \frac{p_y^2}{2\nu} + \frac{p_z^2}{2\nu} - \frac{1}{(x^2+y^2+z^2)^{1/2}}, \qquad (1)$$

where the relevant physical constants such as electric charge, dielectric constant, etc., have been scaled out. There is a rotational symmetry with respect to the x axis, and the corresponding angular momentum M is the only constant of motion apart from the energy. The Hamiltonian is therefore transformed to

$$E = \frac{p_x^2}{2\mu} + \frac{p_r^2}{2\nu} + \frac{M^2}{2r\nu} - \frac{1}{(x^2+r^2)^{1/2}}. \qquad (2)$$

For M different from 0, the phase space is known to be a mixture of hyperbolic regions and stability islands, but, for $M = 0$, and large anisotropy the system appears to be, for all practical purposes, completely hyperbolic. We restrict

 1054-1500/92/010061-09$001.00

ourselves to this case. Setting $M=0$ and renaming r and p_r to stress the two-dimensional nature of the problem, we get the effective Hamiltonian

$$E=\frac{p_x^2}{2\mu}+\frac{p_y^2}{2\nu}-\frac{1}{(x^2+y^2)^{1/2}}. \tag{3}$$

The two dimensional anisotropic Kepler problem is invariant under $C_{2v}=C_2\times C_2$, the group of reflections across the two axes. However, for the $M=0$ restriction of the three-dimensional problem, the y variable is positive (it is the distance from the x axis), there is no x-axis reflection symmetry, and the symmetry group is only C_2, the y-axis reflection symmetry. Using this symmetry, the motion can be reduced to a fundamental domain[8] with $x\geqslant 0$ and $y\geqslant 0$. The three-dimensional nature of the problem also shows up in the Maslov indices, in a way that will turn out to be essential to the convergence of cycle expansions.

A. Scale conventions

The homogeneity of the potential can be used to scale out the energy dependence and bring the action to the form

$$(1/\hbar)S_p(E)=kT_p, \tag{4}$$

where T_p is the period of prime cycle p evaluated for energy fixed to $E=-1/2$, and the wave number k is inverse of the square root of the energy expressed in " Rydberg" units:

$$k=\sqrt{E_R/E},\quad E_R=-\frac{m_0e^4}{2\kappa^2\hbar^2}, \tag{5}$$

and e is the electric charge. The mass unit is normalized by convention to $\mu\nu=1$; all calculations presented here are carried out for the silicon ratio $\mu/\nu=4.810$. The energy shell is customarily fixed to $E=-1/2$. Equation (4) is a consequence of the relation $T=\partial S/\partial E$, with T evaluated for $E=-1/2$. A reader interested in comparing different spectra published in the literature should note that, due to a difference in the definition of the effective Hamiltonian, the Kohn–Lüttinger[9] Rydberg unit E_R^{KL} is related to (5) by $E_R^{KL}=\sqrt{\nu/\mu}E_R$, and the exact eigenvalues in the complex k plane are related to the spectra of Refs. 10 and 2 by $\mathrm{Im}\,k=0$,

$$\mathrm{Re}\,k=\frac{(\mu/\nu)^{1/4}}{\sqrt{-E^{KL}}}. \tag{6}$$

For the anisotropic Kepler problem the stability eigenvalues of a periodic orbit are independent of energy.

III. CYCLE EXPANSIONS

Cycle expansions of dynamical zeta functions have recently been shown to be effective in classical chaos[11] and open quantum systems[3] applications; for hyperbolic dynamical systems with finite grammars, the correlation exponents, dimensions, escape rates, quantum resonances, etc., have been computed to high accuracies with relatively little numerical effort. For example, the escape rate of a chaotic map is given by the leading zero of[12]

$$1/\zeta(z)=\prod_p(1-t_p),\quad t_p=z^{n_p}|\Lambda_p^{-1}|, \tag{7}$$

where the product is taken over the prime (i.e., nonrepeating) periodic orbits p of length n_p and stability Λ_p. In order to evaluate this infinite product, we must use some expansion scheme; cycle expansions in their crudest form attain this by ordering the cycles according to the length of their symbol strings, carrying out the multiplication for cycles up to given cutoff length, and truncating the series to a polynomial in z. For example, for systems with complete binary symbolic dynamics, one obtains

$$\begin{aligned}1/\zeta(z)&=(1-t_0)(1-t_1)(1-t_{01})(1-t_{001})(1-t_{011})\cdots\\&=1-t_0-t_1-(t_{01}-t_0t_1)-(t_{001}-t_0t_{01})-(t_{011}\\&\quad-t_1t_{01})-\cdots.\end{aligned} \tag{8}$$

The important feature of this expansion is that the contributions separate in a finite number of *fundamental cycles* (here t_0 and t_1) and the *curvatures*, combinations of longer cycles shadowed by products of shorter ones:

$$\frac{1}{\zeta}=1-\sum_f t_f-\sum_c t_c. \tag{9}$$

The zeta function appropriate for the evaluation of quantum spectra follows from the Gutzwiller semiclassical trace formula for the Green's function

$$g(e)=g_0(E)+\frac{1}{i\hbar}\sum_p T_p\sum_{n=1}^{\infty}\frac{1}{|J_p^n-I|^{1/2}}e^{in[S_p/\hbar-m_p\pi/2]}. \tag{10}$$

This can be rewritten as

$$g(E)-g_0(E)=\frac{d}{dE}\ln Z(E), \tag{11}$$

with Z for systems with two degrees of freedom given by[13]

$$Z(E)=\prod_p\prod_{k=0}^{\infty}(1-t_p\Lambda_p^{-k}),\quad t_p=\frac{e^{i[S_p/\hbar-m_p\pi/2]}}{|\Lambda_p|^{1/2}}, \tag{12}$$

where S_p is the action, Λ_p is the stability, and m_p is the Maslov index for the prime cycle p.

Discrete symmetries lead to splitting of the spectrum into subspectra belonging to different irreducible representations of the symmetry group. The Z function can be written as a product over the irreducible representations, $\Pi_\alpha Z_\alpha$, with

$$Z_\alpha=\prod_p\prod_{k=0}^{\infty}(1-\chi_\alpha(g_p)t_p\Lambda_p^{-k}), \tag{13}$$

where the product over p refers to prime cycles in the fundamental domain, χ_α is the group character of the representation α, and g_p is the group element that relates the fundamental domain orbit to a segment of the full space orbit.

In the case of the anisotropic Kepler problem the y-axis reflection symmetry splits the eigenvalue spectrum into the even A_1 subspace, and the odd A_2 subspace. The group elements are the identity e and the reflection σ, with the even representation character $\chi_{A_1}(\sigma) = 1$, and the odd representation character $\chi_{A_2}(\sigma) = -1$.

The cycle expansion evaluation of spectra for the anisotropic Kepler problem differs from the Gutzwiller's periodic orbit calculation[14] in several aspects as follows.

(1) The zeta functions that we expand are already asymptotic, arranged in such a way that the spectrum is dominated by short cycles, with long cycles contributing small curvature corrections. In other applications zeta functions have yielded exponentially better convergence than that obtainable from trace formulas.

(2) Symmetries are used to restrict the dynamics to a fundamental domain, factorize the spectra, and simplify the symbolic dynamics (this is, by now, standard, and has been independently done by other groups contributing to this issue of CHAOS[2,5]).

(3) Series of cycles accumulate to limits with finite stability and action, which might cause cycle expansions to diverge. However, our numerical results indicate that the Maslov phases induce cancellations between successive terms in cycle expansions and that the remaining sums are convergent.

IV. SYMMETRIES AND SYMBOLIC DYNAMICS

In order to identify the short fundamental cycles and control the contributions of longer cycles by grouping them into curvature combinations, we need a symbolical description of all possible trajectories of our system. To be useful for cycle expansions, symbolic dynamics must reflect the dynamics in a natural fashion; as we shall see, this requirement leads to symbolic dynamics different from the obvious binary dynamics.

A. Binary symbolic dynamics

An orbit that has just crossed the y axis will, due to the anisotropy, fall faster toward the x axis and thus always cross the x axis before the next y-axis crossing. If we choose the x axis as a Poincaré section, there are two topologically distinct possibilities: Either the orbit has crossed the y axis between successive crossings of the x axis, or it has not. This leads to Gutzwiller's choice of symbolic dynamics for the anisotropic Kepler problem, namely, the sign of x at each crossing of the x axis. At large anisotropy, $\mu/\nu > 9/8$, the orbit can cross the x axis any number of times between two y-axis crossings, and, consequently, any string of symbols (signs of x) can be dynamically realized. Gutzwiller has conjectured[1] that there exists a unique orbit for each infinite symbol sequence. We believe that this is very unlikely; for small anisotropies above 9/8, elliptic islands have been found,[15] and one suspects that such islands exist for all anisotropies; in another model, which has for a long time looked as chaotic, careful symbolic dynamics work has ferreted out stability islands.[16] However, such islands, if they exist for $\mu/\nu \approx 5-20$, are certainly very small and will have a negligible effect on low quantum states. We shall proceed as though the anisotropic Kepler problem is fully chaotic.

Gutzwiller's symbolic dynamics is complete quaternary; any closed orbit must cross the x axis an even number of times, and the four possible combinations of pairs of signs can be used as four letters of a quaternary symbolic dynamics, with the only restriction that the two symbolic fix points, $\overline{++}$ and $\overline{--}$, are not dynamically realizable.

We do not use this quaternary symbolic dynamics, since the convergence of cycle expansions is improved by making full use of the symmetries of the problem and restricting the dynamics to a fundamental domain. We replace the x- and y-symmetry axes by reflecting walls and restrict the motion to a quadrant of the full x-y space. With the x axis as the Poincaré section, the two possible topologically distinct motions between successive bounces off the x-wall are:

$$0 \to \text{no bounce off the } y \text{ wall}$$

and

$$1 \to \text{bounce off the } y \text{ wall.} \tag{14}$$

This yields a binary dynamics description of the orbits of the anisotropic Kepler problem, which is complete, except for one orbit: The fixed point $\overline{0}$ is not realized dynamically. Gutzwiller's global symbolic dynamics $\ldots s_n s_{n+1} s_{n+2} \ldots$ is related to the fundamental domain symbolic dynamics[8] by a simple rule: $a_n = 0$ if $s_n = s_{n+1}$, and $a_n = 1$, otherwise. For example,

$$+ - - - \to 1100,$$

$$+ + + + + - - - - - \to 10000.$$

With simple binary symbolic dynamics, all should be well and ready for numerical computations. However, the curvature expansions[17] presume an approximately linear relationship between symbolic lengths and actions, and symbolic lengths and stability exponents. This assumption is badly violated in the anisotropic Kepler problem, where numerical work indicates that the cycles can be grouped in infinite families, with actions and stabilities converging to finite limits.[18,2] This simplest example of such a family is 10^{n-1}. A cycle of this family bounces along the x axis $n-1$ times, crosses the y axis at the nth bounce and continues at the other side of the origin. As n gets larger, the trajectory hugs closer and closer to the x axis. In particular, the actions of cycles in such sequences converge to the action of the limiting *collision trajectory*.

In the anisotropic Kepler problem, four such collision orbits along the symmetry axes survive from the isotropic case. In the isotropic case they belong to the family of Keplerian ellipses of given action; they are periodic in the sense that they go into the center and return along exactly the same path as they arrived. In the anisotropic case, however, it is not clear whether a sensible continuation through the singularity at the center exists (Yoshida[19] defines it by going into complex time). We provisionally omit collision orbits from our numerical computations, keeping in mind that they do control the limits of converging families of cycles, and that any serious attempt to improve the periodic orbit theory in this problem probably should incorporate them. The action of the collision orbits is given by the third Kepler law:[20]

$$T = 2\pi a^{3/2} m^{1/2}, \tag{15}$$

where m is the mass and a is the major semiaxis. For the anisotropic Kepler problem, this yields

$$T_x = 2\pi(\mu/\nu)^{1/4} = 9.30499\ldots,$$
$$T_y = 2\pi(\nu/\mu)^{1/4} = 4.24271\ldots. \tag{16}$$

Yoshida[19] has given an explicit formula for the stabilities of the collision orbits:

$$\Lambda = (|c| + \sqrt{1+c^2})^2 \text{ with } c = \cos((\pi/2)\sqrt{9-8\mu/\nu}), \tag{17}$$

which yields $\Lambda = 2.35\ldots$ for the x-axis collision orbit, but $\Lambda \approx 10^8$ for the y-axis collision orbit. We have not rederived this formula, and, as far as we can tell, no family converges to the $\Lambda = 2.35\ldots$ stability. It should be mentioned that Wintgen[2] is firmly convinced that the y-axis collision orbit is infinitely unstable, although we know of no evidence for this claim.

B. Infinite symbolic dynamics alphabet

The pruning of the fixed point $\bar{0}$, is usually implemented by replacing the binary alphabet by an unrestricted, but infinite alphabet.[17] As we shall see, this is indeed a natural choice for the anisotropic Kepler problem (and has already been introduced by Devaney[21] in this context).

Numerical investigations of a set of approximately 2000 cycles (though admittedly a small set in the present context, this set is still much larger than any used in previous calculations) have led us to the conclusion that the cycles can be grouped in families of converging stability and action, and that these families are of the form

$$10^{n_1-1}10^{n_2-1}\cdots10^{n_k-1}, \quad n_i \leqslant 2, \tag{18}$$

where the n_i's either go to infinity or are fixed equal to 1. Furthermore, the differences $n_i - n_j$ of those n_i that do go to infinity are to be kept constant, and no two consecutive n_i's must equal 1.

In order to get the symbolic grouping of the cycles in accordance with the physical grouping, we will change our Poincaré section to the y wall. The topologically distinct orbits are now coded by the number of bounces off the x wall between successive bounces off the y wall; that is, we have the natural numbers as our symbols or n-ary dynamics:

$$n \to n \text{ bounces off the } x \text{ wall.} \tag{19}$$

The families of cycles converging to a fixed action and stability are now of the form

$$n_1 n_2 \ldots n_k, \tag{20}$$

with the same restrictions on the n_i's. As examples of families, we have n_1, $1n_1$, $1n_1n_2$, and $1n_11n_2$, but not $2n_1$, $11n_1$ or $n_1(2{*}n_1)$.

With the infinite symbolic dynamics, we have grouped cycles of comparable actions and stabilities into classes of the same symbolic length. But we are now left with the problem of summing infinite series in the cycle expansion of the zeta function. So far, the only organizational principle that seems to work is a pairing of families. The families of (20) can be paired in families that have almost identical actions and stabilities. These are of the form

$$n_1 n_2 \ldots n_k \quad \text{and} \quad 1n_1n_2\ldots n_k. \tag{21}$$

The initial symbol 1 in the second group of families gives rise to a difference in Maslov index of 2. This results in opposite signs on the weights t_p of the zeta function, making the contribution from the two families almost cancel. Here, the three-dimensional nature of the problem is important since the difference is Maslov index for the two-dimensional system would have only been 1.

Cycles from paired families trace almost identical paths in the fundamental domain. For the duration of most of the cycle, the orbits are almost indistinguishable, but, as the cycle from the first family starts to retrace itself, the second will make one small bounce to the x wall and back. This would in the full space be seen as a pseudo semicircle resulting in a 180° turn.

There are two questions to be asked about the limits of these cycle families: What happens when all n_i symbols go to infinity and what happens when the differences $n_i - n_j$ go to infinity? The answers we get from our numerical work seem to be very simple. In the first case, the trajectories approximate collision trajectories along the x axis; in the second case, in addition they approximate collision trajectories along the y axis. Recalling that the stability of the y-collision trajectory was estimated to be of order $\approx 10^8$, it is not surprising that families with diverging $(n_i - n_j)$'s apparently have diverging stabilities. A hope for the future is that we might be able to divide the stability limit of families with constant differences $n_i - n_j$ into two parts: one from the approximations of the x-axis collision orbits and one from shifting between these. If, however, we let the differences $n_i - n_j$ diverge, there will be one more part from approximating the y-axis collision orbits. For the action the picture is even simpler: The limit is the sum of the actions of the limiting collision trajectories.

V. NUMERICAL RESULTS

In a system with a finite alphabet and finite grammar symbolic dynamics, the evaluation of the zeta functions is fairly straightforward. One finds the shortest orbits, multiplies the factors $(1 - t_p)$ for all orbits up to the cutoff length n, truncates the polynomial approximation to the Z function to the same order n, and then numerically deter-

TABLE I. The actions and the stability exponents for the families of cycles with symbolic sequences $n_1 = n$, $n_1n_2 = 1n$, $n_1n_2 = n,n+1$, and $n_1n_2n_3 = 1,n,n+1$. The $n \to \infty$ Kepler law limits for actions are also indicated.

	n		$1n$		$n(n+1)$		$1n(n+1)$	
n	S	$\ln\|\Lambda\|$	S	$\ln\|\Lambda\|$	S	$\ln\|\Lambda\|$	S	$\ln\|\Lambda\|$
2	5.316	1.167	7.496	2.116	14.32	4.103	12.04	3.816
3	7.010	1.679	8.317	2.515	16.25	4.866	14.91	4.649
4	8.020	1.958	8.757	2.636	17.30	5.136	16.55	5.009
5	8.588	2.078	8.999	2.682	17.88	5.224	17.46	5.133
6	8.905	2.120	9.134	2.692	18.20	5.258	17.97	5.174
7	9.081	2.140	9.209	2.703	18.38	5.267	18.25	5.187
8	9.179	2.145	9.251	2.700	18.48	5.274	18.41	5.192
9	9.234	2.151	9.274	2.706	18.53	5.273	18.49	5.193
10	9.265	2.150	9.288	2.701				
11	9.282	2.154	9.295	2.707				
12	9.292	2.151	9.299	2.702				
13	9.298	2.155	9.302	2.707				
14	9.301	2.151	9.303	2.702				
∞	9.305		9.305		18.61		18.61	

mines the zeros of the truncated Z. For the anisotropic Kepler problem, however, the accumulation of infinite families of orbits of approximately the same stability and action makes it uncertain which cycles should be included in this process.

A. Cycle accumulation sequences

The x-axis collision orbit is densely enveloped by infinite sequences of orbits with arbitrarily large numbers of successive x-axis crossings (high $...n_i...$ subsequences). We identify this collision orbit with the $\bar{0}$ fixed point, of the well-defined Kepler period $T_0 = T_x$. Numerical results indicate that the periods of the sequence of orbits $\bar{2}, \bar{3}, ..., \bar{n}$, which twine around the $\bar{0}$ collision orbit, converge to

$$T_n = T_x - b/\rho^n. \tag{22}$$

For $\mu/\nu = 4.81$, $\rho = 1.78...$. Similarly, sequences of cycles of type $2n$ hug closer and closer to an x-collision orbit followed by a y-collision orbit, and their periods converge to $T_y + T_x = 13.5477$ with the same geometric factor. However, the stability exponents in sequences that hug the y axis grow very large with n, as large as for the y-axis collision orbit, and longer cycles can be safely omitted.

Numerical work indicates also that the stabilities of the $\bar{n}$ cycles converge geometrically $\mu_n = \log|\Lambda_n| = \mu_\infty - c/\sigma^n$, although not nearly as smoothly as for the cycle periods. For $\mu/\nu = 4.81$, $\sigma \approx 2$, and $\mu_\infty = 2.15...$.

The first task facing us is to establish whether we can control these families. The families can be paired as

$$n_1n_2...n_k \quad \text{and} \quad 1n_1n_2...n_k, \tag{23}$$

with $n_i \to \infty$ or equal to 1 (no two adjacent n_i's must equal 1) and we will take a look at the two simplest sequences:

$$n \quad \text{and} \quad 1n$$
$$\text{plus} \tag{24}$$
$$n(n+1) \quad \text{and} \quad 1n(n+1).$$

In Table I we give the actions and stabilities of these cycles.

As we can see, the paired families do not converge to exactly the same value for the stability as we would have hoped. It is therefore clear that we cannot include infinitely many members of the families, and a cutoff has to be made. In Table II we show the dependence of the lowest zero of the Z function depending on the cutoff.

It appears that the cutoff does not have significant influence on the zeros of our calculations. We will therefore include the tails up to a finite n_i and hope that this will not distort our results. We have found all cycles, $n_1n_2...n_k$, for $k \leqslant 6$ with $n_i \leqslant 5$. In addition to these, we have included the tails for all families of lengths 1 and 2 and some of length 3, with $n_i \leqslant 10$. In Fig. 1 and Table III we give the results for the periodic orbit quantization compared to the quantum eigenvalues.

B. The functional equation

One obvious shortcoming of the semiclassical cycle expansions is that nothing guarantees the eigenvalues are real, as they should be for a bounded system. A remedy for this failure, the functional equation for the Z function, has been proposed by Berry and Keating[4] and applied to the anisotropic Kepler problem by Tanner *et al.*[2] In our de-

TABLE II. The dependence of the first zero on tail cutoff. We have included tails with $n_i \leqslant n$ for all families of lengths 1 and 2 and some of length 3. Except for an alternation between odd and even n, the value n does not seem to matter, as long as it is larger than 10.

n	E_ζ
6	$1.247 + 0.062\,i$
7	$1.154 + 0.027\,i$
8	$1.238 + 0.069\,i$
9	$1.200 + 0.026\,i$
10	$1.227 + 0.074\,i$
11	$1.222 + 0.054\,i$
12	$1.227 + 0.074\,i$
13	$1.223 + 0.054\,i$
14	$1.227 + 0.074\,i$

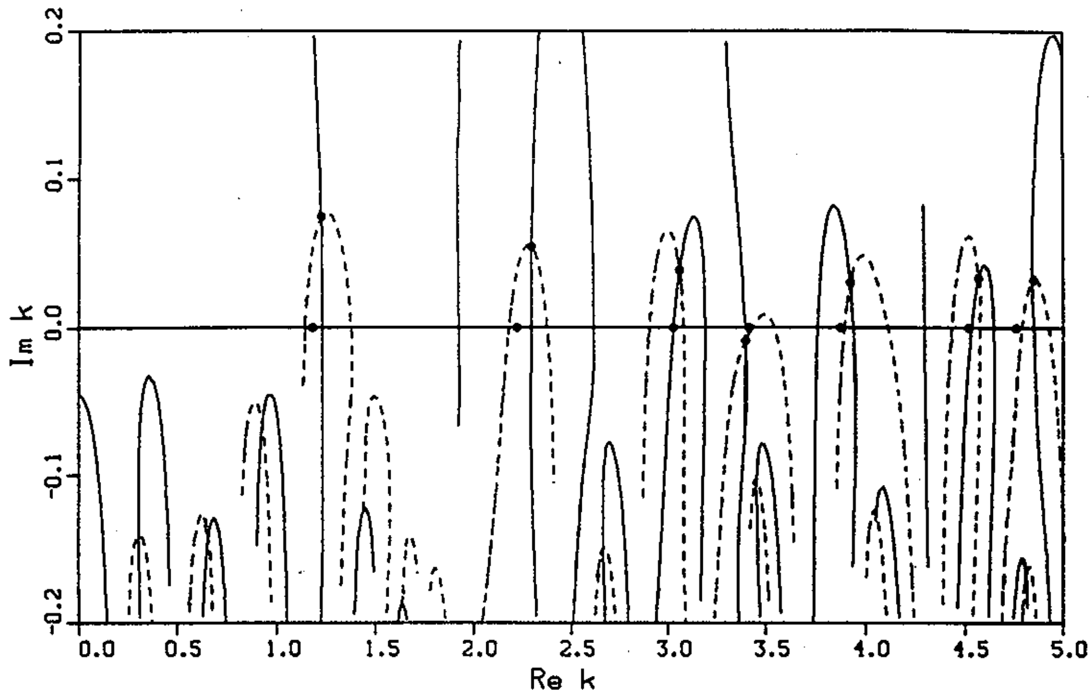

FIG. 1. The Z function for the even subspace A_1. Full lines represent $\mathrm{Re}(Z)=0$; dotted represent $\mathrm{Im}(Z)=0$. The eigenvalues have been marked where they cross. Only the leading eigenvalues have been marked. Quantum eigenvalues are shown as dots on the line $k=0$.

duction of the Z function from Gutzwiller's trace formula, we have disregarded the volume term g_0, and omitted a phase factor $e^{-i\pi\bar{N}}$, where $\bar{N}$ is the integral of the mean level density. Omission of an overall prefactor has no effect on the positions of the zeros of the zeta function, but *were* the zeta function the exact quantum determinant, its inclusion would, in principle, make the Z function real for real values of the energy. "The functional equation" idea is to take the real part of the semiclassical approximation to the quantum determinant, and study only its zeros. In Fig. 2 and Table III we give the results of this computation; $\bar{N}$ is taken from Ref. 2.

TABLE III. The eigenvalue spectrum for the even subspace A_1. The first entry is the "exact" quantum mechanical value,[10] the second is the corresponding zero of the zeta function, and the third is the zero of the functional equation form of the zeta function. The values are related to those of Ref. 2 by a factor of $(\mu/\nu)^{1/4}$. There is no numerical evidence that the eigenvalues are improved by use of the functional equation.

E_{QM}	E_ζ	$E_{\zeta(R)}$
1.183	$1.227+0.074\,i$	1.235
2.222	$2.297+0.054\,i$	2.306
3.026	$3.059+0.038\,i$	3.053
3.415	$3.397-0.009\,i$	3.399
3.875	$3.926+0.030\,i$	3.935
4.518	$4.568+0.033\,i$	4.567
4.761	$4.851+0.032\,i$	4.866
5.316	$5.366+0.016\,i$	5.368
5.474	$5.509+0.019\,i$	5.512
5.844	$5.895+0.018\,i$	5.916
6.130	$6.198+0.027\,i$	6.230
6.466	$6.507-0.004\,i$	6.504

We do not observe any improvement in the accuracy due to the use of the functional equation, although its use led to a considerable reduction of the work needed to find zeros as they are now restricted to the real axis. Furthermore, while in the complex plane one has to distinguish between the leading and the nonleading zeros, here this ambiguity is postulated away.

C. A naive cycle product

It has been suggested by Martin Sieber[5] that one may forgo the cycle expansions altogether by evaluating the real part of the unexpanded truncated product representation of the functional determinant. This is a very violent approximation to the true zeta functions, as all of its complex zeros are wrong; surprisingly, this too produces a reasonable spectrum. In Fig. 3 we see, however, that, even though we still obtain the energy spectrum to the same accuracy, the Hamburg "zeta function" (of Ref. 5) is very kinky and plagued by false zeros.

D. Irreducible cycles

The exponent proliferation of periodic orbits is one of the major obstacles when one wants to improve a calculation using the cycle expansion technique. Eu. Bogomolny[6] has proposed a way to reduce the number of orbits necessary when calculating a zeta function to a given accuracy. The idea is to keep successively redefining the alphabet and assuming perfect shadowing of the cycles in the new alphabet. Bogomolny conjectures that it suffices to leave out most of the longer, "shadowed," cycles and to keep only the subset of the *irreducible* cycles.

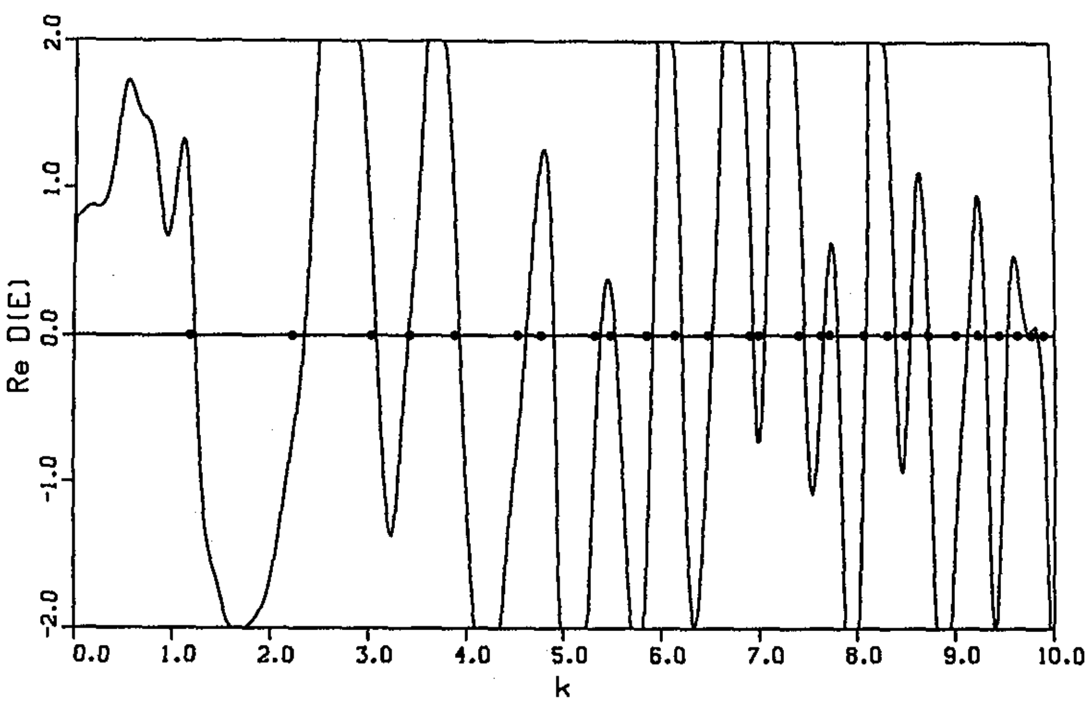

FIG. 2. The real part of $e^{-i\pi\bar{N}}Z(k)$ for real k for the even subspace A_1. The quantum mechanical spectrum is given by the dots. Notice the smooth behavior of the curve compared to Fig. 3.

Since we are not by any means satisfied with the accuracy of the spectrum of the anisotropic Kepler problem calculated from standard cycle expansions, we do not find the anisotropic Kepler problem the optimal system to test this conjecture. Since the conjecture is based on essentially topological arguments, it should apply equally well to simpler systems; we test the conjecture on a one-dimensional map with complete binary dynamics:

$$f(x)=2x+\epsilon x(\tfrac{1}{2}-x),\quad 0\leqslant x\leqslant\tfrac{1}{2},$$
$$f(x)=2x-1-\epsilon(\tfrac{1}{2}-x)(1-x),\quad \tfrac{1}{2}<x\leqslant 1. \tag{25}$$

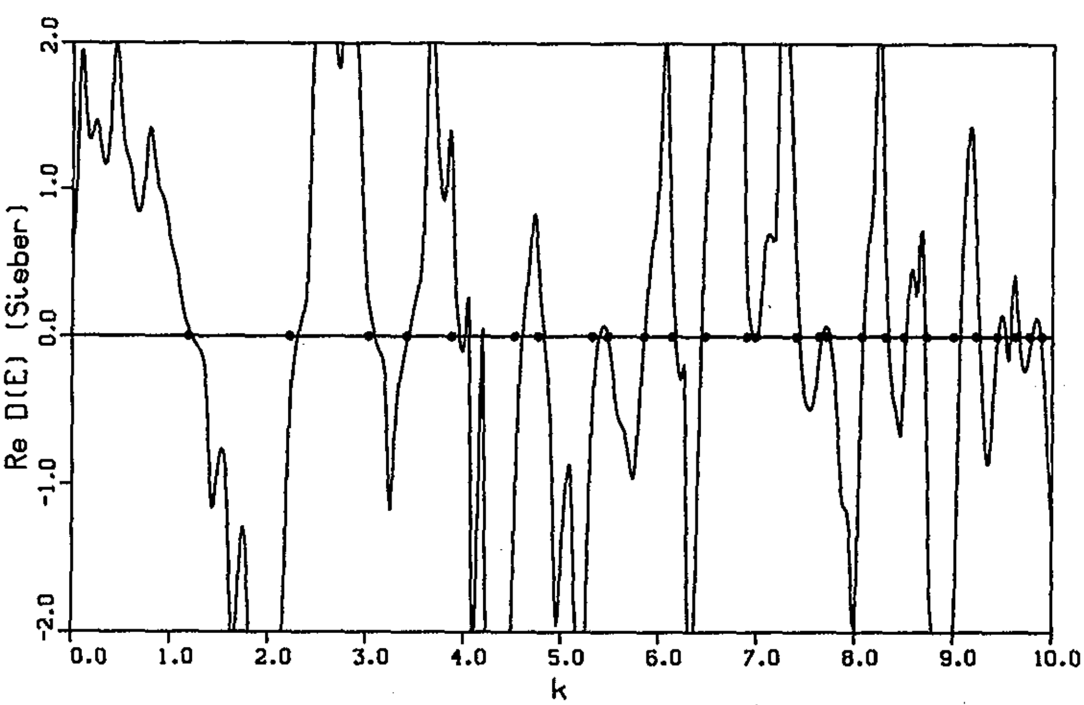

FIG. 3. Using the functional equation on the naive product $\Pi_p(1-t_p)$. The spectrum is reproduced, but the function is much more spiky than for the cycle expanded case, giving rise to false zeros around $k=4$ and $k=9.5$.

TABLE IV. The escape rate computed by prime and irreducible cycles. Columns are: 1, max cycle length; 2, number of cycles used; 3, escape rate; 4, level of the alphabet for irreducible cycles; 5, max cycle length; 6, number of cycles used; and 7, escape rate.

Prime cycles			Irreducible cycles			
n	#	e^{γ}	level	n	#	e^{γ}
3	5	0.94	1	4	6	1.0074
4	8	1.00402	2	8	19	1.00086
5	14	0.999931	3	16	179	1.0002
6	25	$1+4\times10^{-7}$				
7	41	$1-4\times10^{-10}$				
8	71	$1-9\times10^{-13}$				

By construction, the classical escape rate for this map is exactly 0, and the deviation of the leading zero of

$$Z(z)=\prod_{k=0}^{\infty}\prod_{p}\left(1-\frac{z^{n_p}}{|\Lambda_p|\Lambda_p^k}\right) \tag{26}$$

from 1 tests the quality of the cycle expansion truncation. (In the above formula the second product is taken either over prime cycles or over irreducible cycles). The numerical results are given in Table IV. There is no indication that the irreducible cycles approach improves the accuracy-to-work ratio. On the contrary, our numerical studies indicate that the error is dominated by the shortest cycles omitted, with the inclusion of longer irreducible cycles playing a superfluous role.

To understand in more detail how the irreducible cycles work, we have studied the curious way in which they probe the phase space. In the usual cycle expansions if one looks at all periodic points with period less than a given length, one expects them to be rather evenly distributed. The irreducible cycles, however, have a highly uneven distribution. This can be illustrated by plotting their distribution for the Hamiltonian baker's map (stretch by a factor of 2, refold). In Fig. 4, we have marked all periodic points belonging to the irreducible cycles of level 4, i.e., cycles up to length 32. Their number is of order of 10^6 points. Since already 10^5 points distributed evenly would have given a completely black picture, the strong concentration of irreducible points in certain areas is evident.

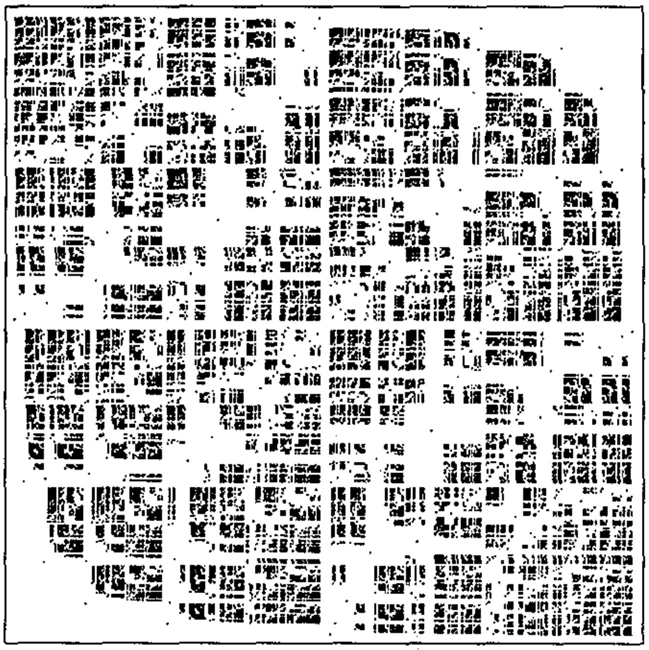

FIG. 4. Irreducible cycles in the baker's map. All irreducible cycles of level 4 (up to length 32) are marked. The white regions are close to short irreducible orbits.

VI. CONCLUSION

Although the numerical results are not unreasonable, we find all of the applications of cycle expansions to the anisotropic Kepler problem deeply unsatisfactory. The sums over infinite families that converge to combinations of collision trajectories are at best conditionally convergent, and not under control yet. Clearly, some more serious analytic work needs to be done, and new methods for resumming such infinite families need to be developed.

In retrospect, Gutzwiller seems to have been very lucky; the central difficulty of the periodic orbit theory in the anisotropic Kepler problem, accumulation of infinite series of orbits to the collision orbits, was not even noticed at the low cycle lengths at which the original calculation stopped. There is a quick fix, and the very first test[18] of cycle expansions yielded accuracy comparable to Gutzwiller's from a handful of cycles. Indeed, Tanner and Wintgen's, Gutzwiller's, and our calculations suggest that almost any method, no matter how cockeyed, easily produces a spectrum of comparably mediocre accuracy. However, in cycling business, one expects not comparable accuracy, but many decades of extra precision for the same effort.

Serious improvements of the convergence, however, still elude us and seem to require a new idea. In our humble opinion, the zeta function calculations presented at the Nordita 1991 Quantum Chaos workshop do not seem to offer any clear evidence in support of the proposed Berry and Keating functional equation, Bogomolny's reduction of cycle expansions, and Sieber's unexpanded truncated Selberg products, without detracting from the inspirations these ideas have for us.

ACKNOWLEDGMENTS

We acknowledge stimulating exchanges with B. Eckhardt, P. Dahlqvist, J. P. Keating, H. H. Rugh, G. Russberg, M. Sieber, G. Tanner, and D. Wintgen. PC is grateful to the Carlsberg Foundation for support, to Edificio Celi for hospitality in Milano, and to M. C. Gutzwiller for many illuminating discussions and support at the I.B.M.T.J. Watson Research Center.

[1] M. C. Gutzwiller, *Chaos in Classical and Quantum Mechanics* (Springer, New York, 1990), and references therein.
[2] G. Tanner and D. Wintgen, CHAOS 2, 53 (1992).
[3] P. Cvitanović and B. Eckhardt, Phys. Rev. Lett. 63, 823 (1989).
[4] M. V. Berry and J. P. Keating, J. Phys. A 23, 4839 (1990); J. P. Keating, CHAOS 2, 15 (1992).
[5] M. Sieber, CHAOS 2, 35 (1992).

[6]Eu. Bogomolny, CHAOS 2, 5 (1992).
[7]B. W. Levinger and D. R. Frankel, J. Phys. Chem. Solids **20**, 281 (1961); J. C. Hensel, H. Hasegawa and M. Nakayama, Phys. Rev. **138**, 225 (1965).
[8]P. Cvitanović and B. Eckhardt, "Symmetry decomposition of chaotic dynamics," submitted to Nonlinearity.
[9]W. Kohn and J. M. Lüttinger, Phys. Rev. **96**, 1488 (1954).
[10]D. Wintgen, H. Marxer, and J. S. Briggs, J. Phys. A **20**, L965 (1987).
[11]R. Artuso, E. Aurell, and P. Cvitanović, Nonlinearity **3**, 361 (1990).
[12]D. Ruelle, *Statistical Mechanics, Thermodynamics Formalism* (Addison-Wesley, Reading, MA, 1978).
[13]A. Voros, J. Phys. A **21**, 685 (1988).
[14]M. C. Gutzwiller, Physica D **5**, 183 (1982).
[15]R. Broucke, in *Dynamical Astronomy,* edited by V. Szebehely and B. Balasz (Univ. of Texas, Austin, 1985), pp. 9–20.
[16]P. Dahlqvist and G. Russberg, Phys. Rev. Lett. **65**, 2837 (1990).
[17]R. Artuso, E. Aurell, and P. Cvitanović, Nonlinearity **3**, 325 (1990).
[18]P. Cvitanović, in *Applications of Chaos, Electrical Power Research Institute Workshop 1990,* edited by J. H. Kim and J. Stringer (Wiley, New York, 1992).
[19]H. Yoshida, Celestial Mech. **40**, 51 (1987).
[20]J. Kepler, *Harmonice Mundi* (Linz, Germany, 1619).
[21]R. Devaney, J. Diff. Eqs. **29**, 253 (1978); Invent. Math. **45**, 221 (1978); Springer Lecture Notes in Math. **597**, 271 (1977).
[22]M. C. Gutzwiller, J. Math. Phys. **12**, 343 (1971).